0026-895X/04/6603-635–647$20.00
MOLECULAR PHARMACOLOGY
Copyright © 2004 The American Society for Pharmacology and Experimental Therapeutics
Mol Pharmacol 66:635–647, 2004

Vol. 66, No. 3
638/1171386
Printed in U.S.A.

A Vascular Endothelial Growth Factor Receptor-2 Kinase Inhibitor Potentiates the Activity of the Conventional Chemotherapeutic Agents Paclitaxel and Doxorubicin in Tumor Xenograft Models

Stuart Emanuel, Robert H. Gruninger, Angel Fuentes-Pesquera, Peter J. Connolly, Jennifer A. Seamon, Susan Hazel, Rose Tominovich, Beth Hollister, Cheryl Napier, Michael R. D'Andrea, Michael Reuman, Gilles Bignan, Robert Tuman, Dana Johnson, David Moffatt, Mark Batchelor, Anne Foley, James O'Connell, Rodger Allen, Martin Perry, Linda Jolliffe, and Steven A. Middleton

Cancer Therapeutics Research (S.E., R.H.G., A. F.-P., P.J.C., J.A.S., M.R., G.B., L.J., S.A.M.) and Oncology Research (R.To., M.R.D., R.Tu., D.J.], Johnson & Johnson Pharmaceutical Research and Development, Raritan, New Jersey; Institute of Medical and Veterinary Science, Adelaide, Australia (S.H.); Piedmont Research Center, Morrisville, North Carolina (B.H., C.N.); and Celltech Research, Limited, Slough, United Kingdom (D.M., M.B., A.F., J.O., R.A., M.P.)

Received March 19, 2004; accepted June 9, 2004

ABSTRACT

Inhibition of angiogenesis may have wide use in the treatment of cancer; however, this approach alone will not cause tumor regression but may only slow the growth of solid tumors. The clinical potential of antiangiogenic agents may be increased by combining them with conventional chemotherapeutics. 4-[4-(1-Amino-1-methylethyl)phenyl]-2-[4-(2-morpholin-4-yl-ethyl)phenylamino]pyrimidine-5-carbonitrile (JNJ-17029259) represents a novel structural class of 5-cyanopyrimidines that are orally available, selective, nanomolar inhibitors of the vascular endothelial growth factor receptor-2 (VEGF-R2) and other tyrosine kinases involved in angiogenesis, such as platelet-derived growth factor receptor, fibroblast growth factor receptor, VEGF-R1, and VEGF-R3, but have little activity on other kinase families. At nanomolar levels, JNJ-17029259 blocks VEGF-stimulated mitogen-activated protein kinase signaling, proliferation/migration, and VEGF-R2 phosphorylation in human endothelial cells; inhibits the formation of vascular sprouting in the rat aortic ring model of angiogenesis; and interferes with the development of new veins and arteries in the chorioallantoic membrane assay. At higher concentrations of 1 to 3 μM, this compound shows antiproliferative activity on cells that may contribute to its antitumor effects. JNJ-17029259 delays the growth of a wide range of human tumor xenografts in nude mice when administered orally as single-agent therapy. Histological examination revealed that the tumors have evidence of reduced vascularity after treatment. In addition, JNJ-17029259 enhances the effects of the conventional chemotherapeutic drugs doxorubicin and paclitaxel in xenograft models when administered orally in combination therapy. An orally available angiogenesis inhibitor that can be used in conjunction with standard chemotherapeutic agents to augment their activity may have therapeutic benefit in stopping the progression of cancer and preventing metastasis.

The vascular endothelial growth factor receptor-2 (VEGF-R2) mediates the process of angiogenesis by inducing the survival, proliferation, and migration of endothelial cells (Millauer et al., 1993). Angiogenesis is prominent during embryonic development, but in a normal adult, it occurs only as a result of injury or during endometrial turnover. However, several pathological conditions initiate the growth of new blood vessels, including diabetic retinopathy, age-related macular degeneration, endometriosis, rheumatoid ar-

Article, publication date, and citation information can be found at http://molpharm.aspetjournals.org.
doi:10.1124/mol.104.000638.

ABBREVIATIONS: VEGF-R2, vascular endothelial growth factor receptor-2; PDGF-Rβ, platelet-derived growth factor receptor-β; EGF-R, epidermal growth factor receptor; FGF-R, fibroblast growth factor receptor; HASMC, human aortic smooth muscle cell; HUVEC, human umbilical vein vascular endothelial cells; PLC-γ, phospholipase C-γ; CDK, cyclin-dependent kinase; HER2, human epidermal growth factor receptor-2; FGF-R2, fibroblast growth factor receptor-2; CAM, chorioallantoic membrane; JNJ-17029259, 4-[4-(1-amino-1-methylethyl)phenyl]-2-[4-(2-morpholin-4-yl-ethyl)phenylamino]pyrimidine-5-carbonitrile; MAP, mitogen-activated protein; DMSO, dimethyl sulfoxide; PBS, phosphate-buffered saline; ERK, extracellular signal-regulated kinase; ANOVA, analysis of variance; SU5416, semaxanib; E64, *trans*-epoxysuccinyl-L-leucylamino(4-guanidino)butane; ZD6474, [*N*-(4-bromo-2-fluorophenyl)-6-methoxy-7-[(1-methylpiperidin-4-yl)methoxy]quinazolin-4-amine]; PTK787, (1-[4-chloroanilino]-4-[4-pyridylmethyl] phthalazine succinate).

thritis, and the vascularization of primary and secondary tumors (Folkman, 1995). Specific inhibitors of VEGF-R2 activity might have potential therapeutic benefit in managing these conditions. The growth of solid tumors beyond the size of a few millimeters in diameter depends on the ability to recruit new blood vessels from the existing vascular network (Folkman, 1972).

Among the stimulators of neovascularization, the VEGF family (VEGF-A, VEGF-B, VEGF-C, and VEGF-D) and their corresponding tyrosine kinase receptors [VEGF-R1 (Flt-1), VEGF-R2 (Flk-1; KDR), and VEGF-R3 (Flt-4)] play a central role in the angiogenic process (Ferrara, 1999). Expression of the VEGF receptors is restricted primarily to endothelial cells in which the VEGF ligands exert mitogenic, chemotactic, and permeability effects that are mediated through the VEGF receptor tyrosine kinases (Mustonen and Alitalo, 1995). Binding of VEGF-A or -B to VEGF-R1, or VEGF-A, -C, or -D to VEGF-R2, or VEGF-C or -D to VEGF-R3 leads to receptor dimerization, tyrosine autophosphorylation, and signal transduction. In the case of VEGF-R2, stimulation by VEGF activates multiple signal transduction pathways, including phosphorylation of phospholipase C-γ (PLC-γ), mitogen-activated protein kinase, glyceraldehyde-3-phosphate, and selected Src and Shc isoforms, leading to the formation of Shc-Grb2 and Nck complex formation (Waltenberger et al., 1994; Kroll and Waltenberger, 1997). Biological activities such as mitogenic and chemotactic responses of endothelial cells, along with changes in endothelial cell morphology, increased permeability, and membrane ruffling, are principally mediated through VEGF-R2 activation of MAP kinase via the PLC-γ, protein kinase C, and raf-1 mitogen-activated protein kinase kinase pathways and by the p38 kinase in response to VEGF (Rousseau et al., 1997). In contrast, VEGF-R1 does not mediate a mitogenic response in endothelial cells or in transfected cells upon VEGF binding but can induce chemotactic activity in monocytes (Barleon et al., 1996). VEGF-R1 is phosphorylated after ligand binding but induces different signal transduction pathways from VEGF-R2 in transfected cells. The expression level of VEGF in tumor cells has been shown to correlate with tumor growth rate, vascular density, and tumor metastasis (Takahashi et al., 1995). A variety of approaches to blocking VEGF action have been shown to inhibit tumor growth, including neutralizing antibodies to the VEGF ligand (Kim et al., 1993) or the VEGF receptor (Witte et al., 1998), antagonistic VEGF variant proteins (Siemeister et al., 1998), soluble VEGF receptor proteins (Millauer et al., 1994), antisense constructs (Cheng et al., 1996), dominant-negative mutants (Millauer et al., 1996), ribozymes (Ke et al., 1998), and transfection of tumor cells with inducible VEGF expression constructs (Benjamin and Keshet, 1997). Targeting the tumor vasculature is an attractive point of therapeutic intervention because angiogenesis is required for expansion of all solid tumor types. The endothelial cell type is less likely to develop multidrug resistance than genetically unstable cancer cells (Boehm et al., 1997), and, unlike some targeted therapeutic agents, efficacy is independent of the genetic profile of the tumor cell. Directing therapy at the endothelial network gives drugs direct access to the microvasculature target without the need to penetrate through the tumor mass. Bevacizumab (Avastin; Genentech, Inc., San Francisco, CA), a monoclonal antibody to VEGF that was recently approved by the U.S. Food and Drug Administration, has shown encouraging results in clinical trials in which it has demonstrated activity alone and in combination with conventional therapeutic regimens (Kabbinavar et al., 2003; Yang et al., 2003). Blockade of VEGF-R2 can prevent formation of new vessels but does not destroy existing vasculature, so this strategy may not induce the regression of late-stage established tumors (Bergers and Hanahan, 2002). Combining antiangiogenic agents with standard therapies may provide greater therapeutic potential over single-agent regimens (Morioka et al., 2003). Both antibodies and kinase inhibitors directed at the EGF-R have been shown to augment the activity of standard therapeutics (Ciardiello et al., 1999; Bruns et al., 2000), but there are few reports of VEGF-R2 kinase inhibitors able to enhance the activity of cytotoxic agents (Ciardiello et al., 2003). A variety of small-molecule kinase inhibitors targeted at the VEGF-R2 have been developed or are being evaluated in clinical trials, including compounds in the indolinone (Fong et al., 1999), quinazoline (Wedge et al., 2002), and phthalazine (Wood et al., 2000) structural classes. In this report, we describe an orally bioavailable, small-molecule inhibitor of the VEGF-R2 receptor kinase from a novel 5-cyanopyrimidine scaffold and characterize its pharmacological properties to inhibit VEGF-mediated signal transduction, prevent angiogenesis, and inhibit solid-tumor growth in human tumor xenograft models. We also show that administration of JNJ-17029259 enhances the antitumor activity of doxorubicin and paclitaxel in tumor xenograft models in vivo, and this encourages further studies into the clinical benefits of combining VEGF-R2 kinase inhibitors with cytotoxic agents.

Materials and Methods

Reagents. JNJ-17029259 (Fig. 1) was synthesized by Celltech Research, Ltd., and the Cancer Therapeutics Research team (Johnson & Johnson Pharmaceutical Research and Development, LLC). All studies were carried out with the free-base form of the compound. The VEGF-A ($VEGF_{165}$; R&D Systems, Minneapolis, MN) form of the ligand was used to stimulate HUVEC cells. Doxorubicin was obtained from Meiji Seika Kaisha (Tokyo, Japan), and paclitaxel was from NaPro Biotherapeutics (Boulder, CO).

Cell Culture. HUVEC cells were obtained from Cascade Biologicals (Portland, OR) and maintained in endothelial growth medium (Cambrex Bio Science Walkersville, Walkersville, MD) containing low serum growth supplement. For VEGF-stimulated proliferation and migration assays, HUVECs were maintained in Medium 200 (Cascade Biologicals). Human aortic smooth muscle cells (HASMCs) were obtained from Cascade Biologicals and maintained in medium 231 containing smooth muscle growth supplement. MRC-5 normal

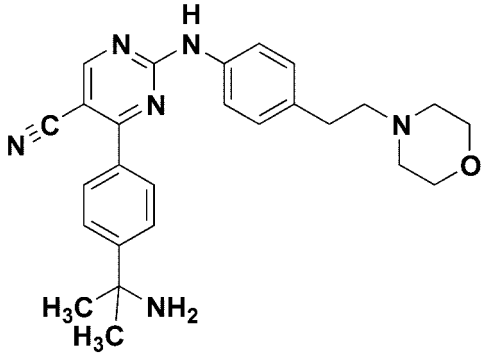

Fig. 1. The chemical structure of JNJ-17029259.

lung fibroblasts, MS1 mouse transformed endothelial cells, and all other cell lines were from the American Type Culture Collection (Manassas, VA). The following human tumor cell lines were used: HeLa (cervical adenocarcinoma), HCT116 (colon carcinoma), SK-OV-3 (ovarian adenocarcinoma), PC-3 (prostate adenocarcinoma), A375 (melanoma), A431 (epidermoid carcinoma), MX1 (breast carcinoma), A2780 (ovarian carcinoma), MV522 (lung carcinoma), and MDA-MB-231 (breast carcinoma). Cell-culture reagents were obtained from Invitrogen (Carlsbad, CA). Cells were maintained at 37°C plus 5% CO_2 as exponentially growing monolayers in the following media supplemented with 10% fetal calf serum (Hyclone, Logan, UT) and 2 mM L-glutamine: HeLa and MDA-MB-231 in minimal essential medium with 0.1 mM nonessential amino acids and 1 mM sodium pyruvate; HCT116 and SK-OV-3 in McCoys 5a; PC-3 in Ham's F-12K; MRC-5 in Eagle's minimal essential medium; and A375 in Dulbecco's modified Eagle's medium with 4 mM L-glutamine and 1.5 g/l sodium bicarbonate.

VEGF Receptor Kinase Assays. Tyrosine kinase activity was measured in streptavidin-coated 96-well scintillation microplates (PerkinElmer Life and Analytical Sciences, Boston, MA) using an N-terminal HIS-tagged soluble rat VEGF-R2 construct expressed and purified from baculovirus. A biotinylated peptide substrate consisting of a fragment of PLC-γ was used as the phosphate acceptor, and inhibition was measured by quantifying the amount of [γ-^{33}P]ATP incorporated into the immobilized peptide in the presence of various concentrations of test compound. VEGF-R2 enzyme was diluted in 50 mM Tris-Cl, pH 8, 10 mM $MgCl_2$, 0.1 mM Na_3VO_4, 1 mM dithiothreitol, 1% DMSO, 0.25 μM peptide substrate, 0.8 μCi/well [γ-^{33}P]ATP (2000–3000 Ci/mmol), and 5 μM ATP in the presence or absence of test compound and incubated at 30°C for 1 h. The reaction was terminated by washing with PBS containing 100 mM EDTA, and plates were counted in a scintillation counter. Linear regression analysis of the percentage of inhibition by test compound was used to determine IC_{50} values (GraphPad Prism 3; GraphPad Software Inc., San Diego, CA).

Selectivity Kinase Assays and Substrates. Assays for inhibition of additional kinases were performed as described for the VEGF-R2 with slight modifications to the assay buffer and different peptide substrates as appropriate for each enzyme. The following N-terminal biotinylated peptides were used: biotin-AEPDYGALY-EGRNPGFYVEANP-amide [VEGF-R2, platelet-derived growth factor receptor-β (PDGF-Rβ), and human epidermal growth factor receptor-2 (HER2)]; biotin-KTPKKAKKPKTPKKAKKL-amide [Cyclin-dependent kinases 1 (CDK1) and 2 (CDK2)]; biotin-poly(GT) 4:1 (insulin receptor kinase, FGF-R2, and EGF-R); biotin-GRTGRRNSI-amide (protein kinase A); biotin-RFARKGSLRQKNV-amide (protein kinase C); biotin-KRRRALS(phospho)VASLPGL-amide (casein kinase 1); biotin-RREEETEEE-amide (casein kinase 2); biotin-KKALRRQETVDAL-amide (calmodulin-dependent protein kinase 2); biotin-KRREILSRRP-(phospho)SYR-amide (glycogen synthase kinase-3); and biotin-APRTPGGRR-amide (MAP kinase ERK-2). The c-kit assay did not use a substrate and measured autophosphorylation activity as described for VEGF receptor autophosphorylation.

Definition and Source of Kinase Enzymes. VEGF-R2 is a fusion protein containing a polyhistidine tag at the N terminus followed by amino acids 786 to 1343 of the rat VEGF-R2 kinase domain (GenBank accession number U93306). CDK1 was isolated from insect cells expressing both the human CDK1 catalytic subunit and its positive regulatory subunit cyclin B (New England Biolabs, Beverly, MA). CDK2 in complex with cyclin A is commercially available (Upstate Biotechnology, Lake Placid, NY). Insulin receptor kinase consists of residues 941 to 1313 of the cytoplasmic domain of the β-subunit of the human insulin receptor (BIOMOL Research Laboratories, Plymouth Meeting, PA). Protein kinase A is the catalytic subunit of cAMP-dependent protein kinase A purified from bovine heart (Upstate Biotechnology). Protein kinase C is the γ or β isoform of the human protein produced in insect cells (BIOMOL). Casein kinase 1 is a truncation at amino acid 318 of the C-terminal portion of the rat δ isoform produced in *Escherichia coli* (New England Biolabs). Casein kinase 2 includes the α and β subunits of the human protein produced in *E. coli* (New England Biolabs). Calmodulin-dependent protein kinase 2 is a truncated version of the α subunit of the rat protein produced in insect cells (New England Biolabs). Glycogen synthase kinase-3β is the β isoform of the rabbit enzyme produced in *E. coli* (New England Biolabs). MAP kinase is the rat ERK-2 isoform containing a polyhistidine tag at the N terminus produced in *E. coli* and activated by phosphorylation with mitogen-activated protein kinase kinase 1 before purification (BIOMOL). The epidermal growth factor receptor (EGFR) is purified from human A431 cell membranes (Sigma Chemical, St. Louis, MO). c-kit consists of the intracellular domain of the human receptor with an N-terminal polyhistidine tag (PanVera Corp., Madison, WI). PDGF-Rβ is a fusion protein containing a polyhistidine tag at the N terminus followed by nucleotides 1874 to 3507 of the human PDGF-Rβ subunit kinase domain (accession number M21616). The HER2 construct contains a polyhistidine tag at the N terminus followed by 24 additional amino acids and begins at amino acid 676 (accession number M11730) followed by the remainder of the HER2 cytoplasmic domain.

In Vitro Autophosphorylation of VEGF Receptor. Autophosphorylation of VEGF receptor was determined as described above with the soluble rat VEGF-R2 construct as the only substrate. The VEGF-R2 enzyme was immobilized from the N-terminal His tag by dispensing the reaction mixture into the well of an nitrilotriacetic acid-nickel–coated scintillating microplate (PerkinElmer) and allowing the reaction to proceed at 30°C for 1 h. The reaction was terminated by washing with PBS, and plates were counted in a scintillation counter. Inhibition of the enzymatic activity of the VEGF-R2 was measured by observing a reduced amount of [γ-^{33}P]ATP incorporated into the immobilized enzyme.

Inhibition of Signal Transduction in HUVEC Cells. To measure the ability of compound to inhibit the activation of VEGF-mediated MAP kinase signaling in HUVEC cells, approximately 10^7 cells were seeded and allowed to adhere overnight. Growth medium was removed and replaced with medium containing 0.1% fetal bovine serum, and cells were incubated an additional 24 h. Cells were then incubated with drug or DMSO vehicle alone for 16 h at a final DMSO concentration of 1%. After stimulation with 100 ng/ml human recombinant VEGF-A for 5 min, cells were lysed in 50 mM HEPES, 150 mM NaCl, 0.5% Triton X-100, 8% glycerol, 2 mM Na_3VO_4, 1.5 mM $MgCl_2$, 1 mM EDTA containing the protease inhibitors 4-(2-aminoethyl)benzenesulfonyl fluoride, aprotinin, leupeptin, bestatin, pepstatin-A, and E64, and total protein was quantified with the BCA protein assay (Pierce, Waltham, MA). The phosphorylation state of the MAP kinase protein ERK1/2 isoforms was detected by SDS-polyacrylamide gel electrophoresis analysis of 20 μg of total protein and immunoblotting with antibodies for phospho-specific (Cell Signaling Technology Inc., Beverly, MA) and total (Promega, Madison, WI) MAP kinase protein. To evaluate the effects of the compound on VEGF-R2 phosphorylation in endothelial cells, 3.5×10^4 HUVEC cells were plated in 48-well cell-culture dishes in endothelial growth medium supplemented with 10% fetal calf serum and cultured for 48 h. Serial dilutions of drug in DMSO (or DMSO vehicle for controls) were added, covering the concentration range of 100 μM to 10 nM, and cells were incubated for 90 min at 37°C. Drug-treated or vehicle-treated cells were stimulated with 100 ng/ml VEGF-A for 7 min, and cells were lysed in 50 mM HEPES, 150 mM NaCl, 0.5% Triton X-100, 8% glycerol, 2 mM Na_3VO_4, 1.5 mM $MgCl_2$, 1 mM EDTA containing the protease inhibitors 4-(2-aminoethyl)benzenesulfonyl fluoride, aprotinin, leupeptin, bestatin, pepstatin-A, and E64. The extent of phosphorylation of the VEGF-R2 in cell lysates was determined in 96-well plates coated with a specific capture antibody followed by an antiphosphotyrosine detection antibody, and absorbance was measured at an optical density of 450 nm. The maximum signal was obtained from control wells containing vehicle stimulated with VEGF after subtraction of the background from wells not stimulated

with VEGF. Stimulation of cells with VEGF increased the phosphotyrosine levels of the VEGF-R2 by at least 7-fold. Linear regression analysis of the percentage of inhibition by test compound was used to determine IC_{50} values.

Inhibition of VEGF-Stimulated HUVEC Proliferation and Migration. To evaluate the inhibition of VEGF-stimulated proliferation, HUVEC cells were seeded into 24-well plates at 5×10^4 cells/well. Experimental compounds were tested at 0.001, 0.01, 0.1, 1, and 10 μM. The negative control corresponded to basal medium alone (medium 200 + 0.5% bovine serum albumin). The positive control and all experimental groups were treated with basal medium supplemented with VEGF (20 ng/ml), and all groups were set up in triplicate. After an incubation period of 72 h at 37°C, cell monolayers were harvested, and cells were counted. To evaluate the inhibition of VEGF-stimulated migration, HUVEC cells were seeded into fibronectin-coated transwells in a 24-well format. The effect of the experimental compounds on VEGF-induced migration was tested at 0.001, 0.01, 0.1, 1, and 10 μM. The negative control corresponded to basal medium alone (medium 200 + 0.2% bovine serum albumin). The positive control and all experimental groups were treated with basal medium supplemented with VEGF (10 ng/ml) added to the lower chamber of the wells, and all groups were set up in triplicate. After a 4-h incubation period at 37°C, cells on the top side of the transwell membrane were scraped with a cotton swab, and cells on the under side of the transwell membrane (migrated cells) were stained with calcein AM. Fluorescent images of migrated cells were obtained under 4× magnification using an Olympus 1X-70 microscope (Olympus, Tokyo, Japan). Five fields were analyzed per transwell.

Cell Proliferation Assays. General antiproliferative activity of VEGF-R kinase inhibitors was assessed in monolayer cultures by [^{14}C]thymidine incorporation into cellular DNA. In brief, 5×10^3 cells were plated into 96-well scintillating microplates (Cytostar-T; Amersham Biosciences UK, Ltd., Little Chalfont, Buckinghamshire, UK) in appropriate culture medium and allowed to adhere for 24 h under standard culture conditions. Cells remained in logarithmic growth phase during the period of the assay and did not reach confluence. Twenty-four hours after plating, test compound was added, and cells were incubated for an additional 24 h. After this incubation, 0.2 μCi/well [^{14}C]thymidine was added and allowed to incorporate into cellular DNA for 24 h, after which time the plate was washed with PBS and counted in a scintillation counter. Total time that cells were exposed to drug was 48 h.

Rat Aortic Ring Assay. The in vitro rat aortic ring assay was performed according to the method described by Nicosia and Antonetti (1990), and the degree of inhibition of vascular sprouting was quantified with an image-analysis program as described previously (Nissanov et al., 1995). In brief, thoracic aorta were freshly isolated from 1- to 2-month-old Sprague-Dawley rats, and 1-mm long sections were embedded in 1.5% agarose-coated six-well plates in gels of fibrin. Serum-free MCDB 131 medium (Caisson Laboratories, Sugar City, ID) was added to the wells, and the cultures were incubated at 37°C in 5% CO_2. Explants generate branching microvessels over a 7- to 14-day period. Vehicle (DMSO) or test compound was added over a concentration range of 0.001 to 10.0 μM on day 0 and again together with fresh media on days 2 and 5 of culture. Microvessel growth was quantified on day 8 of culture and expressed as microvessel area (pixels^2). The percentage of inhibition of microvessel area of drug-treated rings compared with vehicle-treated control rings was calculated using the mean values for each treatment group. Statistical differences between experimental groups were analyzed by ANOVA and Dunnett's t test, with a P value of 0.05 or less considered statistically significant. Linear regression analysis of the percentage of inhibition by test compound was used to determine IC_{50} values.

Early Chorioallantoic Membrane Assay. The early chorioallantoic membrane (CAM) assay is a modification of the classic chicken CAM assay and was performed as described previously (Hazel, 2003). In brief, fertilized chicken eggs were incubated for 3 days at 39.5°C, and embryos were cracked from the eggshell and placed in an incubation apparatus containing DMEM growth medium. On day 4, embryos were photographed at 5× magnification under a dissecting microscope, digital images were captured, and the area of the CAM was measured with image-analysis software. Embryos were divided into treatment groups, and drug or vehicle was applied on 5- to 8-mm methylcellulose discs that were placed on top of the CAMs. After an incubation period of 18 to 24 h, contrast agent dissolved in skim milk was injected into the CAM with a 30-gauge needle, and images were captured at 5× and 63× magnification. Vein lengths, artery lengths, and CAM areas were determined from the 5× image. Vein diameters were measured from images at the 63× magnification. Statistical analysis was performed using ANOVA followed by Student-Newman-Keuls method of multiple comparisons. Where data were not normally distributed, ANOVA on ranks was performed.

Histological Analysis of PC3 Tumors. Tumors from a PC3 xenograft model were established to 0.15 cm^3 before initiation of dosing. The control group was treated with vehicle, and the experimental group was treated for 30 days with 100 mg/kg JNJ-17029259. Tissues were collected and fixed in PBS containing 10% buffered formalin and were routinely processed for paraffin embedding. Sections (5 μm) were placed on microscopic slides for the progressive polychromatic hematoxylin and eosin stain, which stains red blood cells bright red (Sheehan and Hrapchak, 1980). Tumor sections showing no signs of necrosis, which approximately represented the center area of the tumor, were analyzed for red blood cell content per unit area using computer-assisted image analysis [Olympus BX-50 (Olympus); Sony 3CCD DKC-5000 camera (Sony Corporation, Tokyo, Japan); Image Pro version 4.1.0.9, Media Cybernetics, San Diego, CA]. In brief, image-analysis values were set to measure the bright red-stained red blood cells in tissues, which were analyzed in a blinded fashion. In particular, red blood cells were identified through the software to determine the total area occupied by red blood cells, which was obtained as a function of area density. These values were calibrated by comparing the negative control slides to the stained slides. As an additional control, all of the captured tissue images for the analysis were stored with identical photographic settings. Analysis was performed under low magnification using a 10× objective lens (final magnification, 150×). Three scanning areas per animal (n = 4 per group) were selected from areas of the tumor that had obvious regions of red blood cells. Data were calculated as a percentage of the amount of red blood cell staining in the total tissue area (total area of positive pixels/total number of pixels) and subjected to Student's t test statistical analysis using SigmaStat and plotted using SigmaPlot (both from SPSS Inc., Chicago, IL).

Tumor Xenograft Models. Female *nu/nu* mice (Harlan, Indianapolis, IN), aged 9 to 10 weeks, were fed ad libitum water and an irradiated standard rodent diet. Mice were housed in static microisolators on a 12-h light cycle at 21 to 22°C and 40% to 60% humidity. All procedures complied with recommendations of the *Guide for Care and Use of Laboratory Animals* and followed the guidelines set forth by the Association for Assessment and Accreditation of Laboratory Animal Care. Mice were implanted subcutaneously with 1-mm^3 tumor fragments or 5×10^6 cells in the right hind flank. Animals were pair-matched on day 1 when their tumors were in the 40- to 126-mg range. Estimated tumor weight was calculated using the following formula: tumor weight (in milligrams) = $(w^2 \times l)/2$, where w = width and l = length in millimeters. JNJ-17029259 was administered orally in 0.5% methylcellulose containing 0.1% polysorbate 80 in sterile water. Doxorubicin was prepared in saline and administered intravenously. A stock solution of paclitaxel was prepared in 50% ethanol and 50% Cremophor and diluted 10-fold into 5% dextrose in water before intravenous dosing. The tumor growth delay method was followed, where each animal was euthanized when its neoplasm reached a predetermined size. The predetermined "cutoff" tumor size varied for each cell line and was set at 2000 mg for A375, A431, and A2780; 1500 mg for MX1 and HCT116; and 1000 mg for PC3 and

MV522. The mean tumor growth delay in days was calculated by subtracting the mean time to endpoint of the vehicle-treated group from the mean time to endpoint of drug-treated groups. The endpoint was the maximum tumor size permitted for each model. Compound dosing was carried out for 30 to 45 days on various schedules of administration, as indicated in Table 5. Once dosing ceased, tumor measurements continued until all animals in each group reached the endpoint. Data were collected out to days 58 to 65, depending on the model, for any animals remaining on study. Animals were weighed twice weekly during the study, and mice were examined frequently for clinical signs of any adverse, drug-related side effects. All statistical analyses were conducted at P level of 0.05 (two-tailed). Prism (GraphPad) version 3 was used for all statistical analysis and for graphic presentation.

Results

Inhibition of VEGF-R2 Kinase Activity In Vitro. JNJ-17029259 (Fig. 1) represents a novel class of 5-cyanopyrimidine kinase inhibitors and inhibits the activity of the rat and the human VEGF-R2 kinase domain with similar potencies. IC_{50} values of 25 and 21 nM, respectively, were obtained for phosphorylation of the PLC-γ peptide in the rat or poly(GT) substrate in the human assay. In these in vitro kinase assays, JNJ-17029259 exhibits potency superior to the comparator compounds SU-5416, ZD-6474, and PTK787 (Table 1). When substrate was omitted in an in vitro autophosphorylation assay, JNJ-17029259 inhibited autoactivation of the VEGF-R2 with potency similar to the substrate-based assays (IC_{50} of 16 $\pm$ 3 nM) (data not shown), indicating that this compound acts directly on the VEGF-R2 to interfere with its activity and not through interaction with the substrates used in the kinase assay.

In Vitro Kinase-Selectivity Profile. To characterize the selectivity of inhibition, JNJ-17029259 was tested for activity against a representative panel of tyrosine and serine/threonine kinases. The general procedure used to assay for kinase activity was the same as that used in the primary VEGF-R2 screen, except each assay used a different biotinylated peptide substrate, and some buffer components varied slightly for each protein kinase. Known inhibitor compounds appropriate for the kinase being assayed were also included on each plate as internal controls. Among the kinase activities examined, JNJ-17029259 showed selectivity for inhibition of receptor tyrosine kinases involved in angiogenesis, with significant activity on the VEGF-R1, VEGF-R3, and FGF-R1 and some inhibition of the PDGF-Rβ, all of which have essential functions in neovascularization. ZD-6474 is a more

TABLE 1

In vitro activity of JNJ-17029259 and other VEGF-R2 kinase inhibitors

Inhibition of kinase activity was determined in vitro with rat or human recombinant enzymes. VEGF-stimulated phosphotyrosine content of the VEGF-R2 was evaluated in HUVEC cells. Data represent the mean ($\pm$ S.E.) of four separate experiments.

Compound	IC_{50}			
	Rat VEGF-R2 Kinase Activity	Human VEGF-R2 Kinase Activity	VEGF-R2 Phosphorylation in HUVEC Cells	Rat Aortic Ring Assay
		nM		
JNJ-17029259	25 $\pm$ 6	21 $\pm$ 0.6	52 $\pm$ 14	50 $\pm$ 34
SU-5416		220[a]	884[a]	
ZD-6474		40[b]	2673[a]	
PTK787		42[a]	16[a]	675[c]

[a] Data from Manley et al. (2002).
[b] Data from Wedge et al. (2002).
[c] Data from Wood et al. (2000).

TABLE 2

IC_{50} values for in vitro selectivity of JNJ-17029259 and other VEGF-R2 kinase inhibitors

Kinase	JNJ-17029259	SU-5416	ZD-6474	PTK787
		μM		
VEGF-R1	0.090 $\pm$ 0.009	0.043[a]	0.90[a]	0.077[c]
VEGF-R3	0.012 $\pm$ 0.003	0.050[a]	0.233[a]	0.195[a]
Tie2	1.95 $\pm$ 0.07	>10[a]	0.567[a]	>10[c]
PDGF-Rβ	0.27 $\pm$ 0.09	2.22[a]	0.477[a]	0.580[c]
FGF-R1	0.10 $\pm$ 0.02	>10[a]	2.31[a]	>10[c]
FGF-R2	0.172 $\pm$ 0.004			
FLT3	0.23 $\pm$ 0.05			
c-kit	>100	0.660[a]	0.343[a]	0.730[c]
CDK1:cyclin B	4.80 $\pm$ 0.41	>10[a]	>10[a]	>10[c]
EGF-R	>100	>10[a]	0.016[a]	>10[c]
HER2	2.09 $\pm$ 0.57		>20[b]	
Protein kinase-A	>100			
Protein kinase-Cγ	28.3 $\pm$ 2.88			
Protein kinase-Cβ2	>100			
Casein kinase-1	36.76 $\pm$ 0.88			
Casein kinase-2	>100			
Calmodulin kinase-2	24.52 $\pm$ 1.97			
GSK3β	1.31 $\pm$ 0.1			
ERK2 (MAP kinase)	>100			
Insulin-R kinase β	>100			

[a] Data from Manley et al. (2002).
[b] Data from Wedge et al. (2002).
[c] Data from Wood et al. (2000).

potent inhibitor of the EGF-R than the VEGF-R2 and is approximately 10-fold less potent on the VEGF-R1 than the other compounds (Tables 1 and 2).

Inhibition of Signal Transduction by JNJ-17029259 in HUVEC Cells. To determine whether JNJ-17029259 is able to penetrate into cells and block VEGF-mediated signal transduction, HUVEC cells were treated for 16 h with 1 or 10 μM JNJ-17029259. Cells were then stimulated with VEGF, and cell lysates were prepared. Lysates were examined by Western blot with a phosphorylation state-specific antibody to the ERK1/2 isoforms of MAP kinase, a key mediator of biological activity after VEGF stimulation (Waltenberger et al., 1994; Takahashi et al., 1999). The VEGF-induced activation of ERK1/2 phosphorylation in HUVEC cells was completely inhibited by treatment with 1 or 10 μM JNJ-17029259 (Fig. 2), indicating that this compound effectively blocks signal transduction induced by the VEGF growth factor. In cells treated with vehicle only, VEGF stimulation resulted in phosphorylation of ERK1/2 protein (Fig. 2). Blots were also probed with an antibody to total ERK1/2 to show the amount of protein present in each lane, and the protein load was approximately equal for all treatment conditions. We next determined whether treatment of HUVEC cells with JNJ-17029259 could block the VEGF-stimulated phosphorylation of the VEGF-R2. Cells were incubated for 90 min with drug or vehicle and stimulated with VEGF, and lysates were evaluated for phosphotyrosine levels of the VEGF-R2 in a sandwich enzyme-linked immunosorbent assay as described under *Materials and Methods*. As shown in Table 1, JNJ-17029259 inhibited tyrosine phosphorylation of the VEGF-R2 in HUVECs after stimulation with VEGF ligand with an IC_{50} value of 52 $\pm$ 14 nM. For comparison, reported IC_{50} values for the inhibition of VEGF-stimulated phosphorylation of the VEGF-R2 in HUVEC cells by SU-5416, ZD-6474, and PTK787 (Manley et al., 2002) are shown in Table 1. These VEGF-R2 inhibitors were assayed under conditions similar to those described here. The potency of JNJ-17029259 compares favorably with these VEGF-R2 kinase inhibitors, and this shows that the compound is able to reach its intracellular target and prevent activation of the VEGF-R2 in endothelial cells.

Effects of JNJ-17029259 on VEGF-Induced HUVEC Proliferation and Migration. The effect of JNJ-17029259 on VEGF-stimulated HUVEC cell proliferation was determined. Although treatment of HUVEC cells with increasing concentrations of JNJ-17029259 showed a trend toward inhibition of VEGF-stimulated proliferation, this effect was not statistically significant because of the small window of proliferation induced by VEGF treatment. The group treated with 10 μM JNJ-17029259 does not reflect inhibition of VEGF-stimulated proliferation but rather is probably caused by toxicity of the compound, which occurs at this concentration, because growth was inhibited below the basal level seen in the absence of VEGF stimulation in the "NO VEGF" negative control group (Fig. 3A). JNJ-17029259 prevented the VEGF-induced migration of HUVEC cells with inhibition of cell migration observed at all concentrations tested down to 1 nM, and these results were statistically significant (Fig. 3B). Some general toxicity was apparent at the highest concentration tested (10 μM) but to a lesser degree in this assay than seen in the HUVEC proliferation assay because of the shorter 4-h incubation period of the migration assay. Separate positive and negative controls were run for each compound evaluated.

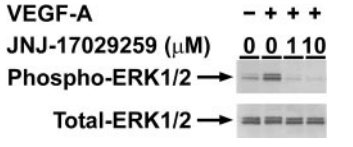

Fig. 2. Inhibition of VEGF-dependent phosphorylation of ERK1/2 in HUVECs by JNJ-17029259. Serum-starved HUVECs were either untreated or treated with 1 or 10 μM JNJ-17029259 for 16 h. Cells were stimulated with 20 ng/ml of VEGF, and cell lysates were subjected to Western blot analysis to detect phosphorylated ERK1/2 (phospho-ERK1/2) or total ERK1/2 (total-ERK1/2). Lane 1 cells were not treated with drug and were not stimulated with VEGF, and they show the basal level of phosphorylation after being serum-starved for 16 h. Lane 2 cells were not treated with drug but were stimulated with VEGF for 5 min to induce phosphorylation of ERK1/2. Cells in lanes 3 and 4 were treated with 1 and 10 μM JNJ-17029259, respectively, and show inhibition of ERK1/2 phosphorylation after drug treatment. Representative data are shown.

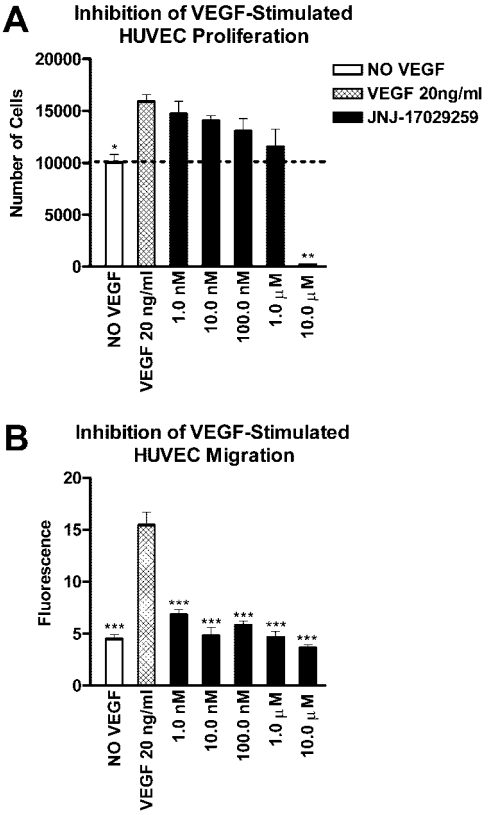

Fig. 3. Effect of JNJ-17029259 on VEGF-stimulated HUVEC proliferation and migration. A, inhibition of proliferation. Controls were either unstimulated (NO VEGF) or stimulated (20 ng/ml VEGF) with VEGF-A and allowed to grow for 72 h. The ability of the compound to inhibit cell proliferation at concentrations from 1 nM to 10 μM was determined. The basal level of growth observed in the absence of VEGF (NO VEGF) is indicated by the broken line. Inhibition of cell growth below the level of the NO VEGF control group indicates toxicity. Cell number was determined from direct cell counts. All groups were set up in triplicate, and the data presented are means; bars, S.E. B, inhibition of migration. Controls were either unstimulated (NO VEGF) or stimulated (20 ng/ml VEGF) with VEGF-A and allowed to migrate for 4 h. The ability of the compound to inhibit cell migration at concentrations from 1 nM to 10 μM was evaluated. After an incubation period of 4 h at 37°C, migrated cells were harvested and stained with calcein AM. Fluorescent images of migrated cells were obtained under 4× magnification using an Olympus 1X-70 microscope. Five fields were analyzed per transwell. All groups were set up with $n = 10$, and the data presented are means; bars, S.E. Statistical significance was evaluated by comparing the NO VEGF negative control or the drug-treated groups with the VEGF-induced positive control group using a two-tailed Student's t test. ⋆, $P < 0.05$; ⋆⋆, $P < 0.01$; ⋆⋆⋆, $P < 0.001$.

Effects of JNJ-17029259 on Cell Proliferation. The antiproliferative activity of JNJ-17029259 was assessed with cell proliferation assays in various human cancer cell lines and on primary MRC-5 human lung fibroblasts, HASMC, and HUVEC cells. These assays were intended to investigate the effect of the compound on cell growth that is unrelated to the inhibition of the VEGF-R2. The IC_{50} value for inhibition of cell proliferation by test compound was measured by incorporation of [^{14}C]thymidine into cellular DNA. JNJ-17029259 exhibited an antiproliferative effect on cell growth, with IC_{50} values in the range of 1 to 3 μM, depending on the cell type (Table 3). Antiangiogenic effects occur at much lower concentrations of compound and are separated from the growth-inhibitory effects observed in this assay. This is illustrated by the difference in the IC_{50} values for inhibition of HUVEC growth in basal medium (2.57 μM) compared with the inhibition of VEGF-stimulated growth (0.1 μM) calculated from the VEGF-stimulated HUVEC proliferation assay (Table 3 and Fig. 3A). To estimate the non-VEGF–specific effects of JNJ-17029259 on mouse endothelial cells, the antiproliferative activity toward the MS1 cell line was evaluated. MS1 is a transformed mouse endothelial line that maintains the phenotypical characteristics of endothelial cells, including expression of Flk-1 (VEGF-R2), factor VIII-related antigen, and uptake of acetylated low-density lipoprotein (Arbiser et al., 1997). Growth of the transformed mouse endothelial cell line MS1 was inhibited in the same concentration range as the other cell types examined (Table 3).

Vascular Sprouting Assay. Compounds were evaluated for the ability to affect the formation of new vessel outgrowth from segments of rat aortic rings embedded in a fibrin gel. JNJ-17029259 suppressed the growth of new vascular processes in this in vitro model of angiogenesis in a dose-dependent fashion with an IC_{50} of 50 ± 34 nM (Table 1). PTK787 has also been reported to inhibit the formation of new vessels in this assay (Wood et al., 2000) with an IC_{50} of 675 nM under similar assay conditions except that capillary outgrowth was measured after day 6 as opposed to day 8 (Table 1).

JNJ-17029259 Treatment in the CAM Assay. Treatment with JNJ-17029259 resulted in reductions in vein and artery length and vein diameter of more than 50% at 20 nM and higher doses (Table 4 and Fig. 4). In the CAMs treated with 50 nM compound, four of six had no remaining blood flow. Total vein length decreased with an IC_{50} of 15.8 nM but was only inhibited a maximum of 30 to 35% at 20 to 50 nM compound. Total artery lengths were reduced with an IC_{50} of 17.8 nM and showed more of a dose response at higher concentrations of 20 to 50 nM JNJ-17029259 reaching a maximum inhibition of 11.7% at 50 nM. CAM growth was reduced to 57% of control in the 50 nM compound group, but this did not reach statistical significance. Vein diameters were significantly reduced in all of the groups treated with 20 nM or higher JNJ-17029259. Examples of CAMs treated with JNJ-17029259 are shown in Fig. 4. At 20 nM compound, there is a large area of hemorrhage in the CAM, and dilated vessel skeletons can be seen at the higher magnification. No blood flow remains in the CAM treated with 50 nM compound, and there are only indistinct vessel remnants seen at the higher magnification.

Inhibition of Human Tumor Xenograft Growth. The antitumor activity of JNJ-17029259 was evaluated in several human tumor xenograft models in nude mice. Compound was formulated in 0.5% methylcellulose containing 0.1% Tween 80 and administered orally. Before initiating treatment, tumors were implanted and allowed to establish growth for 7 to 14 days. Results of these studies are summarized in Table 5 for the various tumor types.

The A375 melanoma cell line was selected because it represents a highly vascular and fast-growing tumor type and has been reported to express VEGF and the VEGF receptor KDR (Liu et al., 1995). In this model, statistically significant efficacy was obtained with daily doses of 100 and 50 mg/kg JNJ-17029259, whereas there was not significant delay of tumor growth at the 25 or 12.5 mg/kg doses (Table 5). For this tumor type, twice-daily dosing did not seem to have any advantage over once-daily dosing with the same cumulative dose when inhibition of tumor size or tumor growth delay was calculated. A375 tumor growth delay results for the 50 and 100 mg/kg once-a-day dose groups are shown in Fig. 5A, showing tumor size, and Fig. 5B, showing the time to end-

TABLE 3
In vitro antiproliferative activity of JNJ-17029259

Cell Line	IC_{50}
	μM
Human cancer cell lines	
HeLa	2.12 ± 0.31
HCT-116	2.74 ± 0.25
SK-OV-3	1.43 ± 0.18
PC3	1.84 ± 0.22
A375	1.28 ± 0.04
MDA-MB-231	2.77 ± 0.73
Normal cell type	
MRC-5	3.43 ± 0.67
HASMC	3.68 ± 0.40
MS1	3.74 ± 0.07
HUVEC non-VEGF–stimulated	2.57 ± 0.47
HUVEC VEGF-stimulated	0.1[a]

[a] Estimated from data in Fig. 3 (n = 3).

TABLE 4
Quantitative measurements of CAM growth from days 4 to 5, vessel lengths, and vein diameter in the early CAM assay

JNJ-17029259 Dose	CAM Growth	Vein Length[b]	Artery Length[c]	Vein Diameter[d]
		%		
DMSO Only	100.0 ± 0.0	100.0 ± 0.0	100.0 ± 0.0	100.0 ± 0.0
5 nM	103.5 ± 20.1	97.8 ± 13.8	101.7 ± 25.7	107.7 ± 25.1
10 nM	97.4 ± 9.7	126.2 ± 15.9	97.3 ± 24.4	108.8 ± 13.1
20 nM	80.1 ± 16.1	29.5 ± 13.7[a]	30.2 ± 12.2[a]	34.4 ± 10.6[a]
30 nM	67.9 ± 13.0	34.6 ± 25.4[a]	16.1 ± 6.3[a]	47.9 ± 16.0[a]
40 nM	79.2 ± 14.2	33.3 ± 18.8[a]	28.8 ± 15.9[a]	30.5 ± 14.8[a]
50 nM	56.7 ± 11.2	32.2 ± 22.4[a]	11.7 ± 8.2[a]	26.4 ± 18.5[a]

[a] $P < 0.05$ vs. DMSO using ANOVA on ranks followed by a Student-Newman-Keuls method of multiple comparisons.
[b] IC_{50} = 15.8 nM.
[c] IC_{50} = 17.6 nM.
[d] IC_{50} = 16.9 nM.

point obtained for these same groups. Time to endpoint refers to the percentage of mice remaining on study and includes only those animals that had tumors smaller than the predetermined cutoff size of 2000 mg. Animals were removed from the study when their tumors reached the cutoff size and were recorded as having died because of cancer.

The PC3 cell line was selected for study as an androgen-independent prostate carcinoma because these tumors as a class can be difficult to treat with standard therapies. Enhanced neovascularization of the PC3 xenografts may also be driven by VEGF secreted by these cells (Ravindranath et al., 2001). JNJ-17029259 slowed the growth of the PC3 tumor in a dose-dependent manner; however, the tumor growth inhibition was less than that seen in the A375 model, although it was still statistically significant at the 100 and 125 mg/kg doses (Table 5). In the A431 epidermoid carcinoma and MX1 breast carcinoma models, optimum efficacy was achieved from an intermittent dosing schedule of 125 mg/kg daily for 4 days followed by 3 days of no dosing. This dosing scheme was carried out for 40 days and resulted in a 61% inhibition of A431 tumor growth, which was not statistically significant, and a 55% inhibition of MX1 tumor growth, which was significant (Table 5). The 50 mg/kg twice-a-day schedule also significantly delayed growth in the A431 tumor model. Other dosing schedules provided some inhibition of A431 and MX1 tumor growth, but the activity was not significant for these models. The A2780 cell type was extremely fast growing, with all of the control animals reaching the study endpoint within 14 days. JNJ-17029259 administered alone did not produce a significant delay of tumor growth in this model. Significant inhibition was obtained after daily treatment with 100 mg/kg JNJ-17029259 in the MV522 lung carcinoma model, and inhibition was seen at 50 mg/kg, but the activity in this group was not statistically significant ($P = 0.06$) (Table 5). Treatment with 10 mg/kg JNJ-17029259 was not sufficient to inhibit HCT116 colon carcinoma growth; however, at 100 mg/kg, there was significant inhibition of tumor growth compared with vehicle-treated animals (Table 5).

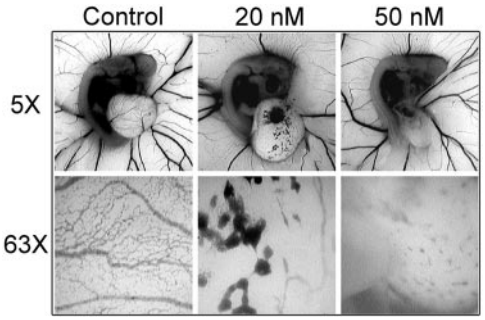

Fig. 4. Effects of treatment with vehicle or JNJ-17029259 in day-5 chicken CAMs. Treatment was initiated on day 4 and completed on day 5. Skim milk plus contrast agent was injected into the CAM to help visualize vessels. Control CAMs were treated with vehicle only. At 20 nM JNJ-17029259, there is a large area of hemorrhage in the CAM at 5× magnification, and dilated vessel skeletons can be seen at the higher magnification of 63×. No blood flow remains in the CAM treated with 50 nM JNJ-17029259, and there are only indistinct vessel remnants even at the higher magnification.

Because noncytotoxic agents will most probably be administered in combination with conventional chemotherapeutics, JNJ-17029259 was evaluated in A431 and MX1 xenograft models administered alone and in combination with doxorubicin. In these studies, doxorubicin was administered at 3 mg/kg i.v. once a day for 5 doses. When administered alone at 125 mg/kg in the A431 model or 100 mg/kg in the MX1 model, JNJ-17029259 demonstrated a nonsignificant inhibition of tumor growth with both of these tumor types (Table 6). When administered in combination with doxorubicin, JNJ-17029259 enhanced the activity of this agent against the A431 and MX1 tumor types (Fig. 6, A and B, and Table 6). The activity obtained with the combination of the two drugs showed significant inhibition of tumor growth that seemed to be additive with no increase in toxicity when 100 mg/kg JNJ-17029259 was combined with 3 mg/kg doxorubicin in the MX-1 study. When a higher dose of JNJ-17029259 was administered in conjunction

TABLE 5

In vivo activity of JNJ-17029259 in human tumor xenograft models

Statistical significance was evaluated by comparing the mean tumor size of vehicle-treated groups with drug-treated groups using a two-tailed Student's *t* test. All dosing was oral with JNJ-17029259 formulated in 0.5% methylcellulose plus 0.5% Tween-80. The percentage of tumor growth inhibition was calculated as the difference between the change in control and drug-treated tumor volumes (T/C) on the last day that all animals were alive in both treatment and control groups. The tumor growth delay in days was calculated by subtracting the mean time to endpoint of the vehicle-treated group from the mean time to endpoint of treated groups. The endpoint was the maximum tumor size permitted for each model as described under *Materials and Methods*.

Tumor Type	Schedule and Dose[a]	Tumor Growth Inhibition[b]	Mean Tumor Growth Delay[c]
		%	*Days*
A375 melanoma	100 mg/kg Q.D. × 45 days	65 (P=0.002)	26.7 ± 7.2
	50 mg/kg Q.D. × 45 days	62 (P=0.005)	13.5 ± 3.1
	50 mg/kg b.i.d. × 45 days	70 (P=0.007)	23.7 ± 3.2
	25 mg/kg b.i.d. × 45 days	34 (P=0.1)	12.2 ± 4
	12.5 mg/kg b.i.d. × 45 days	15 (P=0.52)	2.4 ± 3.4
PC3 prostate carcinoma	125 mg/kg Q.D. × 40 days	56 (P=0.01)	2.3 ± 4
	100 mg/kg Q.D. × 40 days	38 (P=0.004)	8.1 ± 3
	50 mg/kg b.i.d. × 40 days	28 (P=0.16)	4.4 ± 3.5
A431 epidermoid carcinoma	125 mg/kg 4on/3off Q.D. × 40 days	61 (P=0.08)	21.3 ± 4.8
	100 mg/kg Q.D. × 40 days	48 (P=0.07)	16.6 ± 4.2
	50 mg/kg b.i.d. × 40 days	58 (P=0.05)	8.8 ± 3.1
MX1 breast carcinoma	125 mg/kg 4on/3off Q.D. × 40 days	55 (P=0.004)	13.2 ± 4.2
	100 mg/kg Q.D. × 40 days	41 (P=0.11)	13.5 ± 4.8
	50 mg/kg b.i.d. × 40 days	30 (P=0.15)	9.2 ± 3.8
A2780 ovarian carcinoma	100 mg/kg Q.D. × 30 days	6.3 (P=0.06)	1.9 ± 1
MV522 lung carcinoma	100 mg/kg Q.D. × 30 days	54 (P=0.02)	9.1 ± 6.8
	50 mg/kg Q.D. × 30 days	51 (P=0.06)	2 ± 6.7
HCT116 colon carcinoma	100 mg/kg Q.D. × 30 days	45 (P=0.04)	13.8 ± 4.4
	10 mg/kg Q.D. × 30 days	12 (P=0.14)	2.2 ± 2.5

b.i.d., twice per day; Q.D., once per day; 4on/3off, 4 days of dosing followed by 3 days of rest.

with doxorubicin in the A431 study, there was an increase in treatment-related deaths observed over the course of the study, with five of eight animals lost by day 51 after 40 days of dosing with JNJ-17029259 at 125 mg/kg on a 4 days on/3 days off schedule combined with one cycle of doxorubicin administered for 5 consecutive days. JNJ-17029259 was also evaluated when administered in combination with paclitaxel in A2780 ovarian tumor xenografts. The A2780 ovarian cell line is the only cell type examined not reported to express VEGF or its receptor. This tumor type was extremely fast growing, with all untreated and vehicle-treated animals reaching the maximum tumor size within 14 days (Fig. 6C). When administered alone, JNJ-17029259 produced no significant inhibition of tumor growth with 100 mg/kg daily dosing (Table 6). However, when JNJ-17029259 was administered in combination with paclitaxel, there was an enhanced inhibition of tumor growth, which was significant (Fig. 6C and Table 6). The combination of daily dosing with JNJ-17029259 at 100 mg/kg and one cycle of paclitaxel administered every other day for a total of 5 doses at 30 mg/kg, was well-tolerated with no apparent toxicity, and three of six animals experienced a complete regression, having no tumor present upon completion of the study. For all studies

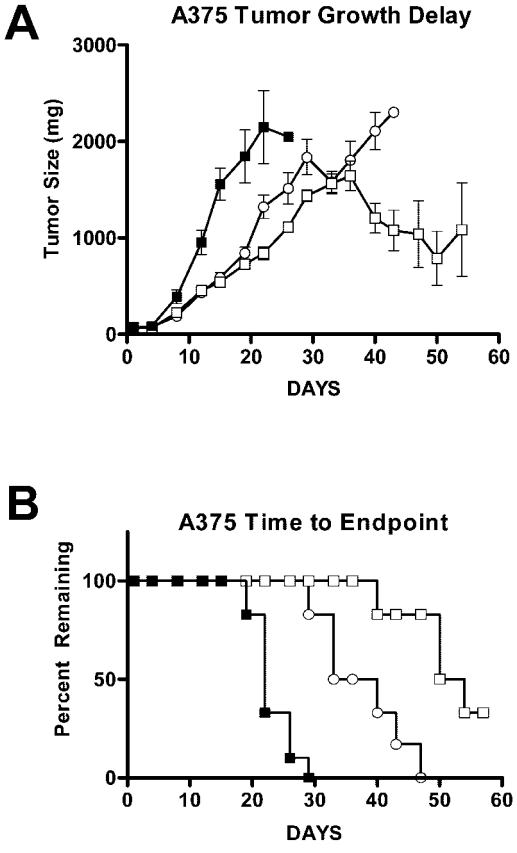

Fig. 5. Inhibition of A375 melanoma xenograft growth by JNJ-17029259. Experimental procedures are described under *Materials and Methods*. In brief, tumor fragments were implanted subcutaneously into female nude mice and allowed to establish to a size of 40 to 126 mg, at which time they were pair-matched into groups; treatment was initiated on day 1. Drug was formulated in 0.5% methylcellulose and administered orally once a day for 45 days. Mice were treated with vehicle (■), 50 mg/kg (○), or 100 mg/kg (□) JNJ-17029259. A, tumor size was measured every 3 days. Values are means; bars, S.E.; $n = 6$. B, survival is indicated as the percentage of animals remaining on study because mice bearing tumors that reached a predetermined cutoff size of 2000 mg were removed from the experiment so that tumors never exceeded 10% of body weight.

TABLE 6
In vivo activity of JNJ-17029259 in human tumor xenograft models dosed in combination with doxorubicin or paclitaxel
Statistical significance was evaluated by comparing the mean tumor size of vehicle-treated groups to drug-treated groups using a two-tailed Student's *t* test. The percentage of tumor growth inhibition was calculated as described in Table 5. The tumor growth delay was calculated as described in Table 5.

Tumor type	Schedule and Oral Dose for JNJ-17029259	Schedule and Intravenous Dose for Second Agent	Tumor Growth Inhibition	Mean Tumor Growth Delay
			%	*days*
A2780 ovarian carcinoma	None	Paclitaxel 30 mg/kg Q.O.D. × 5 days	57 ($P = 0.019$)	12.4 ± 1.1
	100 mg/kg Q.D. × 30 days	None	6 ($P = 0.06$)	1.9 ± 1
	100 mg/kg Q.D. × 30 days	Paclitaxel 30 mg/kg Q.O.D. × 5 days	98 ($P = 0.019$)	31.3 ± 3.1
A431 epidermoid carcinoma	None	Doxorubicin 3 mg/kg Q.D. × 5 days	37 ($P = 0.006$)	11.8 ± 5.1
	125 mg/kg 4on/3off Q.D. × 40 days	None	61 ($P = 0.078$)	21.3 ± 4.8
	125 mg/kg 4on/3off Q.D. × 40 days	Doxorubicin 3 mg/kg Q.D. × 5 days	91 ($P = 0.09$)	N.D.[a]
MX1 breast carcinoma	None	Doxorubicin 3 mg/kg Q.D. × 5 days	48 ($P = 0.03$)	15.2 ± 4.6
	100 mg/kg Q.D. × 40 days	None	41 ($P = 0.11$)	13.5 ± 4.8
	100 mg/kg Q.D. × 40 days	Doxorubicin 3 mg/kg Q.D. × 5 days	96 ($P = 0.01$)	37 ± 2.5

Q.D., once per day; Q.O.D., every other day; 4on/3off, 4 days of dosing followed by 3 days of rest; N.D., not calculated.
[a] This group experienced one case of partial regression and two cases of progressive disease along with five treatment-related deaths.

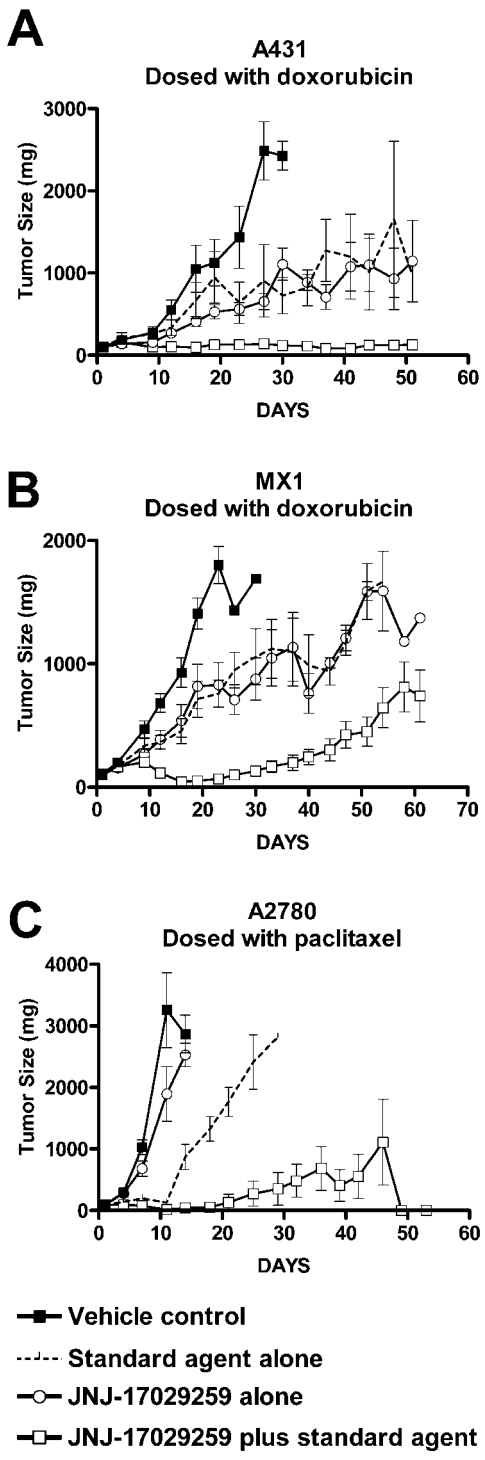

Fig. 6. Effect of JNJ-17029259 on the growth of human tumor xenografts when administered alone and in combination with paclitaxel or doxorubicin. JNJ-17029259 was administered orally in 0.5% methylcellulose containing 0.1% Tween 80. A, in the A431 model, JNJ-17029259 was administered at 125 mg/kg on a 4 days on/3 days off schedule alone (○) or in combination with doxorubicin (□). B, in the MX1 model, JNJ-17029259 was administered at 100 mg/kg/day alone (○) or in combination with doxorubicin (□). Doxorubicin was administered at 3 mg/kg/day i.v. for 5 days in both the A431 and MX1 models (broken line in A and B). Vehicle-treated animals (■) followed the same schedule as JNJ-17029259. C, in the A2780 xenograft model, JNJ-17029259 was administered at 100 mg/kg/day alone (○) or in combination with paclitaxel (□). Paclitaxel was administered at 30 mg/kg/day i.v. every other day for 10 days (broken line in C). Tumor xenografts were established subcutaneously in the right hind flank of athymic mice and allowed to establish to 63 to 256 mg before initiation of treatment. In the A431 and MX1 models, the activity of JNJ-17029259 administered alone was comparable with that obtained with doxorubicin alone. When JNJ-17029259 was administered in combination with doxorubicin, the activity was at least additive. In the A2780 model, JNJ-17029259 had a modest effect when administered alone but enhanced the activity of paclitaxel when the two agents were administered in combination. Data points represent means for eight mice in all treatment groups and 10 mice in vehicle control groups; bars, S.E.

described, groups receiving daily doses of 100 mg/kg JNJ-17029259 alone seemed healthy and experienced an increase in mean body weight over the course of the treatment. Animals receiving paclitaxel or doxorubicin alone did not lose more than 5% of their body weight after treatment with these standard agents, and body weight increased once treatment ceased. Animals receiving JNJ-17029259 plus doxorubicin or paclitaxel experienced a maximum mean body weight loss that did not exceed 16% for any combination, but once chemotherapeutic treatment ended, they progressively gained the weight back and exhibited a net increase in weight at study end. No treatment-related deaths occurred in any of the combination studies with chemotherapeutic agents when JNJ-17029259 was administered at 100 mg/kg.

Histological Effects of JNJ-17029259 in PC3 Xenografts. Analysis of PC3 prostate carcinoma cells grown as xenografts in nude mice showed that there was a significant reduction in the area of red blood cell staining in animals treated once a day for 30 days with 100 mg/kg JNJ-17029259 compared with animals treated with vehicle alone (Fig. 7). Although this is not a direct measure of vascularity, it is evidence of reduced blood supply in treated tumors.

Discussion

This report describes a novel, orally available angiogenesis inhibitor that targets the VEGF-R2 tyrosine kinase. JNJ-17029259 is a potent inhibitor of VEGF-R2–mediated phosphorylation of a peptide fragment of PLC-γ1. PLC-γ1 is an essential component of the signal transduction from the activated VEGF-R2–mediating endothelial cell calcium flux, proliferation, and differentiation (Meyer et al., 2003). The peptide substrate contains amino acids 771 and 783 that are functionally important tyrosine residues in the PLC-γ1 protein. Phosphorylation of PLC-γ1 on tyrosine 783 has been shown to be critical for signaling after PDGF and EGF stimulation (Kim et al., 1991), and this residue is also important for the downstream functions of the FGF and nerve growth factor receptor tyrosine kinases (Rhee, 2001). A direct effect on the activation of the VEGF-R2 is demonstrated by the ability of the compound to interfere with VEGF-stimulated phosphorylation of the VEGF-R2 in HUVEC cells with potency similar to that measured in the substrate-based kinase assay. JNJ-17029259 possesses superior potency to the comparator compounds SU-5416, ZD-6474, and PTK787 against the human VEGF-R2 in substrate-based kinase assays. Experiments to elucidate the mechanism of inhibition of JNJ-17029259 showed that the IC_{50} value increased in proportion to the concentration of ATP in the assay, consistent with an ATP-competitive mode of action (data not shown). Kinase-inhibitor profiling reveals that JNJ-17029259 has good selectivity for the target VEGF-R2 and also inhibits other kinases involved in neovascularization. Inhibition of unrelated kinases such as EGF-R may result in effects not related to

angiogenesis that may be undesirable; however, activity on the FGF-R and PDGF-Rβ that are expressed on endothelial cells and involved in many of the same processes mediated through the VEGF-R2 (Compagni et al., 2000) could contribute to antiangiogenic action. JNJ-17029259, ZD-6474, and PTK787 have activity against PDGF-Rβ, a receptor that can stimulate the mitogenesis and assembly of smooth muscle cells and pericytes into new vessels in conjunction with endothelial cells (Grosskreutz et al., 1999). Inhibition of the VEGF-R1 and VEGF-R3 receptors by JNJ-17029259, which are closely related and in the same family of receptor tyrosine kinases as the VEGF-R2, could confer therapeutic advantages because they are implicated in pathological angiogenesis (Hiratsuka et al., 2001; White et al., 2002).

Treatment of HUVEC cells showed that JNJ-17029259 has the capacity to reach its target in endothelial cells, prevent the autophosphorylation of the VEGF-R2, and block the VEGF-mediated processes of proliferation and migration that are critical for new vessel formation. At the highest concentration assayed (10 μM), JNJ-17029259 exhibited some toxicity in the VEGF-stimulated HUVEC proliferation assay after a 72-h treatment with drug. When tested in vitro in cell-proliferation assays, JNJ-17029259 exhibits some general antiproliferative effects on human cancer cell lines and normal cell types that may be unrelated to inhibition of the VEGF-R2. In the non-VEGF–stimulated HUVEC cell-proliferation assay, the IC_{50} value for inhibition of cell growth was 2.57 μM after a 48-h exposure. The growth-inhibitory effect on the MS1 mouse endothelial cell line was in the same range as for HUVEC human endothelial cells. JNJ-17029259 showed similar potency for slowing the growth of transformed cell lines or normal human cell types, which did not seem to correlate with their expression of the VEGF-R2. However, JNJ-17029259 was 25-fold more potent for inhibition of VEGF-stimulated HUVEC proliferation, for which the IC_{50} was around 0.1 μM. In an in vitro model of vascular sprouting, the compound was able to effectively disrupt angiogenesis, as demonstrated by its inhibition of vascular outgrowth in the rat aortic ring assay, with an IC_{50} of 50 nM. The inhibition of neovascularization from rat aortic rings is probably not caused by an antiproliferative effect on endothelial cells, because the IC_{50} value for this effect is well below the concentration required to interfere with HUVEC cell growth measured in vitro. Treatment with JNJ-17029259 also resulted in a dramatic inhibition of vascular formation in the CAM assay. Vein growth, artery growth, and vein diameter were equally reduced and produced very similar IC_{50} values of 15.8, 16.9, and 17.6 nM, respectively. Various growth factors are implicated in the regulation of angiogenesis in the CAM, such as basic FGF; however, JNJ-17029259 is relatively inactive on the FGF-R2, so its effects in the CAM assay are most probably attributable to interference with VEGF-R-, FGF-R1-, or PDGF-R–mediated processes. Although this compound clearly has antiangiogenic effects at lower concentrations, it also demonstrates antiproliferative effects on cancer cell lines when present at micromolar levels and may be delaying tumor growth in xenograft models by other mechanisms unrelated to its antiangiogenic properties. In fact, plasma levels of 2 to 6 μM are achieved under the 100 mg/kg daily dosing schedule used in the in vivo models (data not shown), and these levels are in the range in which JNJ-17029259 exhibits antiproliferative activity toward cell lines in culture. In PC3 tumor xenografts, there was evidence that treatment with JNJ-17029259 was able to reduce the density of red blood cells present in the tumors, indicating that both antiangiogenic and antiproliferative mechanisms may be contributing to the antitumor activity of this compound.

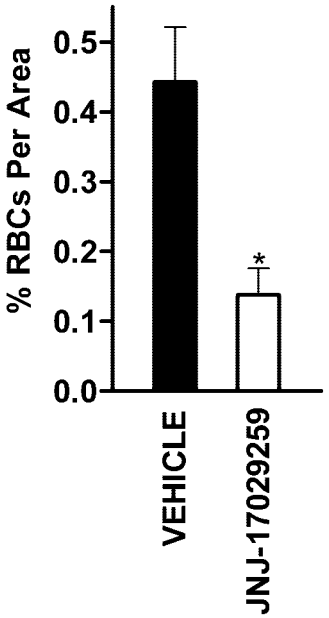

Fig. 7. Vascular density in PC3 tumor xenografts. PC3 tumors ($n = 4$) were allowed to establish to a size of 0.15 cm^3 before initiation of treatment. Tumors were collected from vehicle-treated animals (■) or animals treated with 100 mg/kg JNJ-17029259 once each day for 30 days (□) and fixed in 10% buffered formalin. Histological sections were prepared, and the red blood cells (RBCs) were stained brightly red using an H&E staining method to quantify the percentage of red blood cells per unit area. A significant reduction in the red blood cells per unit area was apparent after treatment with JNJ-17029259 in this tumor type. Data represent the mean ± S.E. of three fields (totaling ~11 mm^2) analyzed for each sample. ⋆, $P < 0.05$ by two-tailed Student's t test.

JNJ-17029259 inhibited tumor xenograft growth after once-a-day oral dosing in a wide range of human cancer cell types. Delay of tumor growth was obtained with more than 50% reduction in mean tumor size in several models including A375, PC3, A431, MX1, and MV522, but tumor regression was not observed. Several of these cell types, such as A375 and PC3, are reported to express both VEGF and the VEGF-R2 and may therefore be stimulating angiogenesis in the mouse xenografts by both autocrine and paracrine mechanisms. The A375 cell line has been shown to respond to VEGF with increased proliferation (Liu et al., 1995). A431 cells secrete VEGF in monolayer cultures and are dependent on it for angiogenesis and growth in vivo (Viloria-Petit et al., 2001). The expression of VEGF by HCT116 cells is critical for their capacity to form tumors in nude mice (Okada et al., 1998), and VEGF production increases under hypoxic conditions in the MX1 cell line (Schmitt et al., 2002). JNJ-17029259 was effective under several schedules, with 50 and 100 mg/kg administered once a day being the most frequently used regimens. When administered at 100 mg/kg on a daily basis, JNJ-17029259 was well-tolerated in all of the in vivo models, with no reduction of body weight and no treatment-related deaths occurring after 30 to 45 days of treatment. Doses lower than 50 mg/kg produced very minimal antitumor effects, whereas doses as high as 125 mg/kg resulted in improved activity; however, prolonged daily dosing at this level could only be tolerated for approximately 30 days, after which time treatment-related deaths began to occur. This

could be avoided by administering the compound at the same high dose but on an intermittent dosing schedule of 4 days of dosing followed by 3 days of rest.

Because VEGF-R2 kinase inhibitors are likely to be administered in conjunction with standard therapies, the ability of JNJ-17029259 to enhance the activity of two chemotherapeutic drugs was evaluated. At the 100 mg/kg dose, the compound was well-tolerated when combined with doxorubicin or paclitaxel in MX1 or A2780 models, respectively, and was able to augment the effects obtained with either agent administered alone. Using the 125 mg/kg intermittent schedule, combination with doxorubicin in the A431 model increased the toxicity observed with higher doses of the compound, indicating that the optimum dose must be determined for each agent to be administered in the combination. Blocking cancer progression by more than one mechanism simultaneously may be an attractive therapeutic approach, with the potential for greater effectiveness over either agent alone (Morioka et al., 2003).

We have described a novel orally available angiogenesis inhibitor able to block VEGF-mediated signaling and inhibit vessel growth both in vitro and in vivo. JNJ-17029259 is a potent inhibitor of several of the receptor tyrosine kinases with roles in angiogenesis including VEGF-R1, -R2, and -R3 as well as FGF-R1 and PDGF-Rβ and probably interferes with the process of vessel formation at multiple levels. This compound exhibits activity at delaying the growth of a variety of solid tumor types when administered alone and is able to augment the activity of conventional chemotherapeutic agents when administered in combination therapy. JNJ-17029259 may also have use for additional indications in which aberrant vascularization is involved, such as diabetic retinopathy and rheumatoid arthritis.

References

Arbiser JL, Moses MA, Fernandez CA, Ghiso N, Cao Y, Klauber N, Frank D, Brownlee M, Flynn E, Parangi S, et al. (1997) Oncogenic H-ras stimulates tumor angiogenesis by two distinct pathways. *Proc Natl Acad Sci USA* **94:**861–866.

Barleon B, Sozzani S, Zhou D, Weich HA, Mantovani A, and Marme D (1996) Migration of human monocytes in response to vascular endothelial growth factor (VEGF) is mediated via the VEGF receptor flt-1. *Blood* **87:**3336–3343.

Benjamin LE and Keshet E (1997) Conditional switching of vascular endothelial growth factor (VEGF) expression in tumors: induction of endothelial cell shedding and regression of hemangioblastoma-like vessels by VEGF withdrawal. *Proc Natl Acad Sci USA* **94:**8761–8766.

Bergers G and Hanahan D (2002) Combining antiangiogenic agents with metronomic chemotherapy enhances efficacy against late-stage pancreatic islet carcinomas in mice. *Cold Spring Harb Symp Quant Biol* **67:**293–300.

Boehm T, Folkman J, Browder T, and O'Reilly MS (1997) Antiangiogenic therapy of experimental cancer does not induce acquired drug resistance. *Nature (Lond)* **390:**404–407.

Bruns CJ, Solorzano CC, Harbison MT, Ozawa S, Tsan R, Fan D, Abbruzzese J, Traxler P, Buchdunger E, Radinsky R, et al. (2000) Blockade of the epidermal growth factor receptor signaling by a novel tyrosine kinase inhibitor leads to apoptosis of endothelial cells and therapy of human pancreatic carcinoma. *Cancer Res* **60:**2926–2935.

Cheng S-Y, Huang H-JS, Nagane M, Ji X-D, Wang D, Shih CC-Y, Arap W, Huang C-M, and Cavenee WK (1996) Suppression of glioblastoma angiogenicity and tumorigenicity by inhibition of endogenous expression of vascular endothelial growth factor. *Proc Natl Acad Sci USA* **93:**8502–8507.

Ciardiello F, Bianco R, Damiano V, De Lorenzo S, Pepe S, De Placido S, Fan Z, Mendelsohn J, Bianco AR, and Tortora G (1999) Antitumor activity of sequential treatment with topotecan and anti-epidermal growth factor receptor monoclonal antibody C225. *Clin Cancer Res* **5:**909–916.

Ciardiello F, Caputo R, Damiano V, Caputo R, Troiani T, Vitagliano D, Carlomagno F, Veneziani BM, Fontanini G, Bianco AR, et al. (2003) Antitumor effects of ZD6474, a small molecule vascular endothelial growth factor receptor tyrosine kinase inhibitor, with additional activity against epidermal growth factor receptor tyrosine kinase. *Clin Cancer Res* **9:**1546–1556.

Compagni A, Wilgenbus P, Impagnatiello M-A, Cotton M, and Christofori G (2000) Fibroblast growth factors are required for efficient tumor angiogenesis. *Cancer Res* **60:**7163–7169.

Ferrara N (1999) Molecular and biological properties of vascular endothelial growth factor. *J Mol Med* **77:**527–543.

Folkman J (1972) Anti-angiogenesis: new concept for therapy of solid tumors. *Ann Surg* **175:**409–416.

Folkman J (1995) Clinical implications of research on angiogenesis. *N Engl J Med* **333:**1757–1763.

Fong TAT, Shawver LK, Tang C, App H, Powell TJ, Kim YH, Schreck R, Wang X, Risau W, Ullrich A, et al. (1999) SU5416 is a potent and selective inhibitor of the vascular endothelial growth factor receptor (Flk-/KDR) that inhibits tyrosine kinase catalysis, tumor vascularization and growth of multiple tumor types. *Cancer Res* **59:**99–106.

Grosskreutz CL, Anand-Apte B, Duplaa C, Quinn TP, Terman B, Zetter B, and D'Amore PA (1999) Vascular endothelial growth factor-induced migration of vascular smooth muscle cells in vitro. *Microvasc Res* **58:**128–136.

Hazel S (2003) A novel early chorioallantoic membrane assay demonstrates quantitative and qualitative changes caused by antiangiogenic substances. *J Lab Clin Med* **141:**217–228.

Hiratsuka S, Maru Y, Okada A, Seiki M, Noda T, and Shibuya M (2001) Involvement of Flt-1 tyrosine kinase (vascular endothelial growth factor receptor-1) in pathological angiogenesis. *Cancer Res* **61:**1207–1213.

Kabbinavar F, Hurwitz HI, Fehrenbacher L, Meropol NJ, Novotny WF, Lieberman G, Griffing S, and Bergsland E (2003) Phase II, randomized trial comparing bevacizumab plus fluorouracil (FU)/leucovorin (LV) with FU/LV alone in patients with metastatic colorectal cancer. *J Clin Oncol* **21:**60–65.

Ke LD, Fueyo J, Chen X, Steck PA, Shi Y-X, Im A-A, and Yung WKA (1998) A novel approach to glioma gene therapy: down-regulation of the vascular endothelial growth factor in glioma cells using ribozymes. *Int J Oncol* **12:**1391–1396.

Kim H-K, Kim J-W, Zilberstein A, Margolis B, Kim J-G, Schlessinger J, and Rhee S-G (1991) PDGF stimulation of inositol phospholipid hydrolysis requires PLC-gamma 1 phosphorylation on tyrosine residues 783 and 1254. *Cell* **65:**435–441.

Kim KJ, Bing L, Winer J, Armanini M, Gillett N, Philips HS, and Ferrera N (1993) Inhibition of vascular endothelial growth factor-induced angiogenesis suppresses tumor growth in vivo. *Nature (Lond)* **362:**841–844.

Kroll J and Waltenberger J (1997) The vascular endothelial growth factor receptor KDR activates multiple signal transduction pathways in porcine aortic endothelial cells. *J Biol Chem* **272:**32521–32527.

Liu B, Earl HM, Baban D, Shoaibi M, Fabra A, Kerr DJ, and Seymour LW (1995) Melanoma cell lines express VEGF receptor KDR and respond to exogenously added VEGF. *Biochem Biophys Res Commun* **217:**721–727.

Manley PW, Furet P, Bold G, Bruggen J, Mestan J, Meyer T, Schnell CR, and Wood J (2002) Anthranilic acid amides: a novel class of antiangiogenic VEGF receptor kinase inhibitors. *J Med Chem* **45:**5687–5693.

Meyer RD, Latz C, and Rahimi N (2003) Recruitment and activation of phospholipase Cγ1 by vascular endothelial growth factor receptor-2 are required for tubulogenesis and differentiation of endothelial cells. *J Biol Chem* **278:**16347–16355.

Millauer B, Longhi MP, Plate KH, Shawver LK, Risau W, Ullrich A, and Strawn LM (1996) Dominant-negative inhibition of Flk-1 suppresses the growth of many tumor types in vivo. *Cancer Res* **56:**1615–1620.

Millauer B, Shawver LK, Plate KH, Risau W, and Ullrich A (1994) Glioblastoma growth inhibited in vivo by a dominant-negative Flk-1. *Nature (Lond)* **367:**576–579.

Millauer B, Wizigmann-Voos S, Schnurch H, Martinez R, Moller NP, Risau W, and Ullrich A (1993) High affinity VEGF binding and developmental expression suggest Flk-1 as a major regulator of vasculogenesis and angiogenesis. *Cell* **72:**835–846.

Morioka H, Weissbach L, Vogel T, Nielsen GP, Faircloth GT, Shao L, and Hornicek FJ (2003) Antiangiogenesis treatment combined with chemotherapy produces chondrosarcoma necrosis. *Clin Cancer Res* **9:**1211–1217.

Mustonen T and Alitalo K (1995) Endothelial receptor tyrosine kinases involved in angiogenesis. *J Cell Biol* **129:**895–898.

Nicosia RF and Antonetti A (1990) Growth of microvessels in serum free matrix culture of rat aorta. *Lab Investig* **63:**115–122.

Nissanov J, Tuman RW, Gruver LM, and Fortunato JM (1995) Automatic vessel segmentation and quantitation of the rat aortic ring assay of angiogenesis. *Lab Investig* **73:**734–739.

Okada F, Rak J, St. Croix B, Lieubeau B, Kaya M, Roncari L, Shirasawa S, Sasazuki T, and Kerbel RS (1998) Impact of oncogenes in tumor angiogenesis: mutant K-ras up-regulation of vascular endothelial growth factor/vascular permeability factor is necessary, but not sufficient for tumorigenicity of human colorectal cells. *Proc Natl Acad Sci USA* **95:**3609–3614.

Ravindranath N, Wion D, Brachet P, and Djakiew D (2001) Epidermal growth factor modulates the expression of vascular endothelial growth factor in the human prostate. *J Androl* **22:**432–443.

Rhee S-G (2001) Regulation of phosphoinositide-specific phospholipase C. *Annu Rev Biochem* **70:**281–312.

Rousseau S, Houle F, Landry J, and Huot J (1997) p38 MAP kinase activation by vascular endothelial growth factor mediates actin reorganization and cell migration in human endothelial cells. *Oncogene* **15:**2169–2177.

Schmitt O, Schubert C, Feyerabend T, Hellwig-Burgel T, Weiss C, and Kuhnel W (2002) Preferential topography of protein regulating vascularization and apoptosis in a MX1 xenotransplant after treatment with hypoxia, hyperthermia, ifosamide and irradiation. *Am J Clin Oncol* **25:**325–336.

Sheehan DC and Hrapchak BB (1980) *Theory and Practice of Histotechnology,* 2nd ed, pp 143–144, Battelle Press, Columbus.

Siemeister G, Schirner M, Reusch P, Barleon B, Marme D, and Martiny-Baron G (1998) An antagonistic vascular endothelial growth factor (VEGF) variant inhibits VEGF-stimulated receptor autophosphorylation and proliferation of human endothelial cells. *Proc Natl Acad Sci USA* **95:**4625–4629.

Takahashi Y, Kitadai Y, Bucana CD, Cleary KR, and Ellis L (1995) Expression of vascular endothelial growth factor and its receptor, KDR, correlates with vascularity, metastasis and proliferation of human colon cancer. *Cancer Res* **55:**3964–3968.

Takahashi T, Ueno H, and Shibuya M (1999) VEGF activates protein kinase C-dependent, but ras-independent raf-MEK-MAP kinase pathway for DNA synthesis in primary endothelial cells. *Oncogene* **18:**2221–2230.

Viloria-Petit A, Crombet T, Jothy S, Hicklin D, Bohlen P, Schlaeppi JM, Rak J, and Kerbel RS (2001) Acquired resistance to the antitumor effect of epidermal growth factor receptor-blocking antibodies in vivo: a role for altered tumor angiogenesis. *Cancer Res* **61:**5090–5101.

Waltenberger J, Claesson-Welsh L, Siegbahn A, Shibuya M, and Heldin CH (1994) Different signal transduction properties of KDR and Flt1, two receptors for vascular endothelial growth factor. *J Biol Chem* **269:**26988–26995.

Wedge SR, Ogilvie DJ, Dukes M, Kendrew J, Chester R, Jackson JA, Boffey SJ, Valentine PJ, Curwen JO, Musgrove HL, et al. (2002) ZD6474 inhibits vascular endothelial growth factor signaling, angiogenesis and tumor growth following oral administration. *Cancer Res* **62:**4645–4655.

White JD, Hewett PW, Kosuge D, McCulloch T, Enholm E, Carmichael J, and Murray JC (2002) Vascular endothelial growth factor-D expression is an independent prognostic marker for survival in colorectal carcinoma. *Cancer Res* **62:**1669–1675.

Witte L, Hicklin DJ, Zhu Z, Pytowski B, Kotanides H, Rockwell P, and Bohlen P (1998) Monoclonal antibodies targeting the VEGF receptor-2 (Flk1/KDR) as an anti-angiogenic therapeutic strategy. *Cancer Metastasis Rev* **17:**155–161.

Wood JM, Bold G, Buchdunger E, Cozens R, Ferrari S, Frei J, Hofmann F, Mestan J, Mett H, O'Reilly T, et al. (2000) PTK787/ZK 222584, a novel and potent inhibitor of vascular endothelial growth factor receptor tyrosine kinases, impairs vascular endothelial growth factor-induced responses and tumor growth after oral administration. *Cancer Res* **60:**2178–2189.

Yang JC, Haworth L, Sherry RM, Hwu P, Schwartzentruber DJ, Topalian SL, Steinberg SM, Chen HX, and Rosenberg SA (2003) A randomized trial of bevacizumab, an anti-vascular endothelial growth factor antibody, for metastatic renal cancer. *N Engl J Med* **349:**427–434.

Address correspondence to: Dr. Stuart Emanuel, Johnson and Johnson Pharmaceutical Research and Development, LLC, 1000 Route 202, Raritan, NJ 08869. E-mail: semanuel@prdus.jnj.com